Journal of Environmental Chemical Engineering 13 (2025) 116978

Contents lists available at ScienceDirect

Journal of Environmental Chemical Engineering

journal homepage: www.elsevier.com/locate/jece

Supercritical CO_2 sterilization for surgical gowns: From disposal towards reuse

María Blanco-Vales [a,1], María Carracedo-Pérez [a,1], Diego Omar Sánchez-Ramírez [b], Alessio Varesano [b], Beatriz Magariños [c], Carlos A. García-González [a,*], Clara López-Iglesias [a]

[a] AerogelsLab, I+D Farma Group (GI-1645), Department of Pharmacology, Pharmacy and Pharmaceutical Technology, Faculty of Pharmacy, iMATUS and Health Research Institute of Santiago de Compostela (IDIS), Universidade de Santiago de Compostela, Santiago de Compostela, E-15782, Spain
[b] CNR-STIIMA (National Research Council of Italy - Institute of Intelligent Industrial Technologies and Systems for Advanced Manufacturing), Corso Giuseppe Pella, 16, Biella BI 13900, Italy
[c] Department of Microbiology and Parasitology, Aquatic One Health Research Center (iARCUS), Faculty of Biology, CIBUS, Universidade de Santiago de Compostela, Santiago de Compostela, 15782, Spain

ARTICLE INFO

Keywords:
Sterilization
Supercritical CO_2
Disposable surgical gowns
Gamma rays
Ethylene oxide
Green technology

ABSTRACT

Surgical gowns (SG) are one of the most used personal protective equipment. As they are mainly intended for single use, they give rise to an enormous amount of waste, posing a major environmental challenge. Sterilization plays an essential role to allow the reuse of such textiles, therefore reducing their massive disposal. Commonly used techniques, such as gas plasma, gamma rays and ethylene oxide, can present important drawbacks regarding biological safety, ecotoxicity, and potential damage to materials. Supercritical CO_2 ($scCO_2$) sterilization emerges as a promising eco-friendly alternative due to the bactericidal properties of CO_2. This work investigates the effectiveness of $scCO_2$ sterilization with disposable surgical gowns (DSG), with hydrogen peroxide as an additive, achieving the required Sterility Assurance Level of $\leq 10^{-6}$. Physical properties and performance of DSG were evaluated after 1, 5, and 10 cycles of $scCO_2$ sterilization and compared to those treated under ethylene oxide and gamma irradiation treatments. Results suggest that $scCO_2$ is a viable, green and reliable option for sterilizing DSG, offering environmental advantages and preserving the functional performance of the material.

1. Introduction

Most personal protective equipment (PPE) are designed for single use, leading to high amounts of waste from healthcare activity [1]. For example, in the USA, perioperative services alone contribute up to 70 % of the solid waste of the hospital, meaning 1.27 million tons of waste annually [2]. Alternative management strategies are needed to tackle this environmental challenge, such as reutilization and/or safe disposal of PPE [1]. In the past, medical waste management used to focus on the treatment of the generated residues, but more attention is now being paid to handling and disposal methods to prevent the spread of diseases and environmental contamination [3]. A safe disposal system implies having trained personnel who can efficiently manage health-related wastes, as well as adequate plans for segregation, disposal, and destruction of residues [4].

Surgical gowns (SG) are PPE classified as Class II medical devices by the United States Food and Drug Administration (FDA) and are used in enormous quantities in hospital environments [5]. SG are the most used PPE after gloves, being worn by healthcare personnel during surgical procedures for protection against body fluids, particulate matter and/or microorganisms [6,7]. Reusable SG are more environmentally friendly than the disposable ones considering four different indicators: natural resource energy (NRE), global warming potential (GWP), blue water (water taken from a water supply and not returned to it), and solid waste [8]. Life cycle assessments for both types of SG determined that reusing a recyclable gown 1000 times instead of using 1000 disposable gowns reduces in 64 % the NRE consumption, 66 % the GWP, 83 % blue water consumption and 84–87 % solid waste generation [8]. Regarding

* Corresponding author.
E-mail address: carlos.garcia@usc.es (C.A. García-González).
[1] These authors equally contributed to this research work

https://doi.org/10.1016/j.jece.2025.116978
Received 10 February 2025; Received in revised form 14 April 2025; Accepted 6 May 2025
Available online 7 May 2025

disposable surgical gowns (DSG) elimination, they are currently either sent to landfills or incinerated, being the former option the most resorted [9].

The use and commercialization of SG is regulated primarily by FDA and Centers for Disease Control and Prevention, which establish the criteria for their manufacture, testing and labeling [10]. Some mandatory requirements for this PPE include a premarket notification to the FDA, which consists of a complete description of the design, materials and intended use; a compliance with Current Good Manufacturing Practice guidelines, ensuring that the SG are of quality and meet FDA standards; and labeling instructions, that indicate the intended use of the PPE, instructions for its use, warning, and precautions. In Europe, SG must follow the regulations set on EN 13795, that establishes their performance, design and labeling, and the Regulation (EU) 2017/745 [11]. As other medical devices, especially those used in surgical procedures, SG must be sterile before use [12]. To achieve their reprocessing and reduce disposal rates, they should be made of materials resistant to the chosen sterilization technique [7]. This implies that their intended protective performance is kept within specifications. Therefore, sterilization plays an important role to achieve such reprocessing, and to differ and reduce the disposal rates. The most common sterilization techniques for PPE are steam heat, dry heat, formaldehyde, peracetic acid, gas plasma, gamma rays (γ-rays), electron beams and ethylene oxide (EO) [1]. For SG, the chosen technique for their sterilization depends on the type of gown (disposable or reusable), as the thermal requirements for non-woven and woven fabrics (used for disposable and reusable gowns, respectively) are different [13]. For DSG, the most common pre-sterilization methods are gas plasma, γ-rays and EO, whereas steam autoclave and dry heat are preferred for reusable SG [8,13]. EO is a chemical sterilizing agent commonly used for processing medical and surgical products when they cannot be sterilized by radiation or heat [14]. However, it produces toxic residues that are highly flammable and should be carefully handled in special facilities. Moreover, it is potentially hazardous to staff and patients, and treatment and aeration times are long (at least 12 h, if not indicated by the manufacturer) [15,16]. γ-rays had been approved for hospital premises due to their highly efficient penetration without leaving toxic chemical residues at mild working temperatures [17]. The high penetrability of γ-rays renders this technique an attractive option for the sterilization of a wide variety of materials, from homo- and heterogeneous liquid and solid systems to disposable medical equipment such as needles, syringes or cannulas. Nevertheless, ionizing irradiation can cause chemical composition changes, a decrease in compressive mechanical properties, and a reduction in molecular weights, particularly in the case of synthetic polymers and biomolecules [18].

New, cost-effective and green technologies are being sought to sterilize new and already used PPE including SG, therefore reducing their massive disposal. Supercritical carbon dioxide ($scCO_2$) sterilization is an innovative and green technology with promising potential in the medical field. On one hand, $scCO_2$ exhibits the characteristic properties of supercritical fluids, behaving like a gas in terms of viscosity and diffusivity, and having a tunable density that can be comparable to that of a liquid. In the case of CO_2, the critical point is reached at mild conditions, i.e. 73.8 bar and 31.0 ºC [19,20]. Besides, CO_2 is a GRAS substance (*Generally Recognized As Safe*) approved by FDA because of its low toxicity, non-flammability, and innocuous nature [20]. Furthermore, CO_2 is a greenhouse gas that contributes to global warming; hence, finding new uses for it is an environmentally friendly valorization practice. In the last 50 years, $scCO_2$ had been proved useful as a treatment to control pathogenic microorganisms in food systems, taking advantage of its biocidal properties [21–23]. In the biomedical field, it has also been proved effective in the inactivation of microorganisms, in sensitive and complex materials such as aerogels, membranes, foams or even drug formulations [24–28].

The inactivation mechanism of $scCO_2$ consists of several steps that are interrelated and occur at the same time [20,29]. Firstly, $scCO_2$ solubilization in the extracellular medium causes its acidification, damaging the cellular membrane. CO_2 also penetrates and accumulates inside the cells, reducing the pH of the intracellular medium. This damages the structure of the cell and interferes with its catalytic and metabolic activities. In addition, CO_3^{2-} anions, present both in the intra- and extracellular environments, precipitate with Ca^{2+} and Mg^{2+}. Lastly, $scCO_2$ may extract vital constituents from the cells, such as lipids and intracellular substances. These effects are sufficient to inactivate most bacteria in vegetative forms. However, in medical devices, a sterility assurance level (SAL) of 10^{-6} is mandatory, meaning that the survival probability is one microorganism in a million for the most resistant microorganism against the sterilization technique. $scCO_2$ itself cannot achieve high levels of inactivation against more resistant microorganisms, such as sporulated forms, so $scCO_2$ needs an additive to achieve this level depending on working conditions (pressure and temperature) including hydrogen peroxide (H_2O_2), acetic acid, tert-butyl hydroperoxide, or even water, for higher pressure and temperature conditions [5, 20, 30–32].

Previous works aiming the standardization of this technology reported that bioindicators (BI) composed of $\geq 10^6$ dry endospores, from EO, γ-rays and steam sterilization techniques were subjected to $scCO_2$ treatment with H_2O_2 as an additive [25,33,34]. These studies concluded that *Bacillus pumilus* dry spores were the most resistant microorganisms to this sterilization methodology, being then established as the BI for this technique. Due to the environmental concerns of PPE waste after SARS-CoV-2 epidemy, various microbial inactivation protocols using $scCO_2$ have been developed. Surgical, cloth, and N95 masks have been evaluated after being subjected to a $scCO_2$ decontamination process against this virus, concluding that this technology could minimize the environmental risk [30]. In the specific case of DSG, other techniques such as steam sterilization and electron-beam irradiation were applied with reusing purposes, but modified the functionality of the materials [35,36]. However, in a recent work, $scCO_2$ treatment successfully inactivated SARS-CoV-2 in SG components without compromising their physicochemical features [37].

In this research paper, a protocol for the complete sterilization of DSG based on $scCO_2$ technology was developed. For the first time, whole DSG were reprocessed in a 2-liter autoclave for 1, 5 and 10 cycles of $scCO_2$ under mild working conditions in terms of temperature (39 ºC), pressure (140 bar) and in the presence of a chemical additive (1100 ppm H_2O_2). *B. pumilus* dry spores were used as the BI in $scCO_2$ sterilization processes to confirm the achievement of a SAL of $\leq 10^{-6}$. Furthermore, the results of DSG sterilized with $scCO_2$ were compared to those of DSG treated by standard sterilization techniques in the medical field (EO and γ-rays). Scanning electron microscopy (SEM), Fourier-transform infrared (FTIR) spectroscopy and differential scanning calorimetry (DSC) analyses of the sterilized DSG were carried out to determine changes in morphology, composition and crystallinity, respectively. The water contact angle (WCA) was assessed, and hydrostatic pressure, tensile and bursting strength tests were also performed to confirm that the treated DSG could pass the standard performance requirement.

2. Materials and methods

2.1. Materials

Surgical gowns UltraGard Standard (E3506CEA, L, 120 cm) were purchased from MEDLINE International (Châteaubriant, France) and had a mass per unit area of 35 $g \cdot m^{-2}$. DSG consisted of one outer layer (*S*) and one inner layer (*S*), both made of spun-bond non-woven fabric, and three middle layers (*M*) made of melt-blown non-woven fabric. This structure is referred to as *SMMMS*. CO_2 (99.8 % purity) was supplied by Nippon Gases (Madrid, Spain), and hydrogen peroxide (H_2O_2) 30 % (w/w) by Sigma-Aldrich (Madrid, Spain).

To avoid contamination once the material was sterilized, the DSG

were packaged in sterilization pouches from Soplaril Hispania (Barcelona, Spain). These pouches are made of polypropylene, polyester, and medical grade paper and designed with a pore size that prevents the penetration of new microorganisms while allowing the performance of sterilant agents in accordance with the standard UNE-EN ISO 11140–1:2015 [38]. Sterility bioindicator *B. pumilus* (ATCC 27142) spore strips (10^6 spores/strip) were purchased from Sigma-Aldrich (Madrid, Spain). Trypto-casein soy agar (TSA) and Trypto-casein soy broth (TSB) media were purchased from BIOKAR Diagnosis (Pantin, France).

The different sterilization treatments were carried out on the entire DSG contained in thermosealed pouches, which guarantee the preservation of sterility once the process is complete and allow the DSG to be handled without contamination issues before being used in surgical procedures.

2.2. Sterilization treatment with $scCO_2$

Entire DSG were placed inside a high-pressure 2-liter autoclave (Eurotechnica GmbH, Bargteheide, Germany). Operating conditions were set based on prior works at 140 bar, 39 °C, constant stirring [27,33], and 1100 ppm of H_2O_2 related to the vessel volume. Various concentrations of H_2O_2 were previously tested, and it was found that with lower amounts of this additive it was not possible to sterilize dry spores of *B. pumilus*. The system was pressurized at 25 g·min^{-1} for 1 h until the desired working pressure was reached, after which the exposure of the material to $scCO_2$ for microbial inactivation in the autoclave was carried out in two steps: a first static step of 2 h without flow of fresh CO_2, and a second dynamic step of 1 h with constant flow of fresh CO_2 (20–25 g·min^{-1}). Before collecting the material, a final depressurization step was performed at 3.5 bar·min^{-1}. To evaluate the recurrent reusability of SG, the samples were subjected to 1, 5, and 10 consecutive sterilization cycles. DSG treated by $scCO_2$ sterilization were denoted as *X*$scCO_2$, where *X* corresponds to the number of sterilization cycles that the DSG was exposed to.

Dry spore strips of *B. pumilus* were placed in thermosealed bags beside the DSG at the top and at the bottom of the autoclave, as well as inside different areas of the DSG for selected cycles. After $scCO_2$ sterilization, spore strips were collected, seeded in tubes containing TSB medium and incubated for 7 days at 37 °C. The absence or presence of bacterial growth was determined by optical evaluation of the turbidity present in the tubes and then confirmed by transferring the liquid to TSA plates, checked every day for 7 days.

2.3. EO sterilization

The EO sterilization process was carried out in a SUOD142483 sterilizer (Suphatec S.L., Bigues i Riells, Spain) following the ISO 11135:2014 [39]. The chemical sterilization was performed during 4 h at 55°C, and with a minimum relative humidity (RH) of 40 %. For cleaning the samples from toxic residues, a ventilating process was carried out that consisted of a first vacuum step of 21 min followed by a flushing of N_2 at 600 mbar during 8 min. Then, a second vacuum step was performed during 12 min. After that, a ventilation step with air was carried out at 600 mbar during 8 min followed by a second air ventilation at 500 mbar during 34 min. The sterile samples (named *EO*) were safely obtained after 48 h of the last aeration step.

2.4. γ-ray sterilization

The γ-ray irradiation was performed in a First-category radioactive facility IR/B-02/69 (Aragogamma S.L., Les Franqueses del Vallès, Spain). The applied dose was 30.6 kGy with a ^{60}Co source at room temperature during *ca.* 8 h, meeting the requirements established in ISO 11137-A2:2020 [40]. Samples sterilized by this method were called *γ-rays*.

2.5. Scanning electron microscopy (SEM)

The morphology of the DSG was evaluated using an X-EVO SEM (Carl Zeiss Microscopy GmbH, Cambridge, UK) with an electron high tension of 20 kV and a working distance of 32 mm. Prior to analysis, samples were coated with a thin film of gold using a Quorum SC7620 sputter-coater (Laughton, UK) with a current of 20 mA for 120 s. The fiber diameter distribution was estimated by Fiji/ImageJ v.1.51 (ImageJ, Madison, WI, USA) using SEM images on two different points for each sample.

2.6. FTIR spectroscopy

Spectra were recorded from 4000 to 650 cm^{-1} with 100 scans and 4 cm^{-1} band resolution by a Thermo Nicolet Nexus spectrometer (Thermo Fisher Scientific Inc., Madison, WI, USA) with an ATR accessory - Smart Endurance (diamond crystal ZnSe focusing element). All spectra were normalized at 2916 cm^{-1}.

2.7. Differential scanning calorimetry (DSC)

DSC analyses were performed using a Mettler Toledo DSC821e (Schwerzenbach, Switzerland) from −50 to 200 °C with a heating rate of 10 °C·min^{-1}. The calorimeter cell was flushed with 100 mL·min^{-1} of N_2 and a mass of ~1.6 mg was used. A baseline correction using the adjacent-averaging smoothing method was performed.

2.8. Water contact angle (WCA)

WCA was measured by an EasyDrop Standard Contact Angle Measuring system supported by DSA1 software (KRÜSS GmbH, Hamburg, Germany). The measurements were carried out thirteen times for each sample at 20 °C and 65 ± 5 % RH using 9.6 μL of MilliQ water (0.5 μS·cm^{-1} and 72 mN·m^{-1}).

2.9. Hydrostatic pressure test

Hydrostatic pressure tests were performed according to AATCC test method 127–2017 [41]. The tests were carried out in a Hydrostatic Head Tester FX 3000 Hydrotester IV (Textest Instruments AG, Schwerzenbach, Switzerland). At least three measurements were done for each sample, and all samples (20 cm × 20 cm) were kept overnight at 20 ± 2 °C and 65 ± 5 % RH before the test. A gradient of 60 mbar·min^{-1} using MilliQ water was employed in a circular test area of 100 cm^2.

2.10. Tensile strength test

Dry and wet tensile strength tests were done according to UNE-EN ISO 29073–3 [42]. For the material testing, a Z005 TH ProLine 5 kN material testing machine (ZwickRoell GmbH, Ulm, Germany) was used. These tests were carried out 5 times in longitudinal and lateral directions. Samples (5 cm × 20 cm) were kept overnight at 20 ± 2 °C (65 ± 5 % RH) before each test. Elongation was set at 100 mm·min^{-1}. In wet conditions, samples were immersed in an aqueous solution with a nonionic surfactant (1 g Tween 20, 1 g·L^{-1}) for 1 h before conducting the measurements.

2.11. Bursting strength test

Bursting strength tests in dry and wet states were performed according to EN ISO 13938–1:2020 using TruBurst Pneumatic Bursting Strength Tester (James H. Heal Co. Ltd., Halifax, UK) [43]. The test area was 10 cm^2 and five specimens were used on both sides (internal and external). In the dry state, samples were kept overnight at 20 ± 2 °C (65 ± 5 % RH) before each test. In wet state, samples were treated according to EN 29073–3, i.e. in the same way as for the tensile strength

test.

2.12. Statistical analysis

All results were expressed as mean ± standard deviation. Statistical analyses of melting temperature (T_m), crystallinity, peak ratio, WCA, hydrostatic pressure, tensile and bursting strengths and strains of the DSG were performed using one-way ANOVA test, with subsequent Tukey's multiple comparison test using GraphPad Prism v.8.0.2 software (GraphPad Software, San Diego, CA, USA).

3. Results

3.1. Evaluation of the sterilization efficacy of the batches using $scCO_2$

The sterilization procedure using $scCO_2$ was carried out in two sequential steps to guarantee its maximum efficacy. The static step (i.e. in the presence of $scCO_2$ and stirring, but in absence of flow) enhanced the homogenization of the additive in the atmosphere of $scCO_2$, while during the dynamic step (i.e., in the presence of $scCO_2$ with flow), the additive is removed from the material, and lipids are extracted from the membranes of weaker microorganisms, like vegetative cells [20,44]. A single static step would result in possible material incompatibility, as the residual additive would remain on it as well as in the vessel, which could be dangerous for both the operator and the person who would use the SG. During the dynamic step, CO_2 environment was designed to be renewed at least two times before depressurizing the system. Since the effectiveness of each sterilization batch process must be rigorously evaluated, the spore strips of *B. pumilus* were individually thermosealed in the same type of pouches as those used for the DSG and located in two different positions in the autoclave (one at the top and the other at the bottom) to ensure process homogeneity and the absence of dead points in the pressurized vessel. In some of the tests, sterility was also checked by placing the spore strips inside the pouches containing the DSG and found to be sterile. The implemented supercritical sterilization procedure was considered as sterilizing (SAL of $\leq 10^{-6}$) since no bacterial growth was observed on the TSA plates after the incubation time for any of the spore strips placed in the autoclave during the corresponding sterilization batch.

3.2. Physicochemical evaluation of the DSG after the different sterilization treatments

No visible alterations were observed in DSG compared to the blank sample, such as shrinkage in dimensions, scratches in the textile, or changes in color, when inspected with the naked eye after any of the sterilization techniques.

Morphological changes at microscopical level were evaluated by SEM analysis. *SMMMS* structure was confirmed (Fig. S1), in which the outer and inner layer (*S*) are composed of fibers and the middle layers (*MMM*) of microfibers. *SMMMS* is a typical non-woven fabric used in the fabrication of PPE like DSG due to its high productivity and cost-effectiveness; furthermore, this non-woven fabric is widely employed in the medical field because of its mechanical and protection properties against infective agents in blood or body fluids [45]. These fibers/microfibers can be manufactured by using polyolefins like polypropylene (PP) with a polyethylene (PE) coating over PP *S*-layers. *Blank* DSG consisted of fibers in the 15 – 25 μm size range and microfibers in the 0.5 – 7 μm size range. The control sample (*Blank*) was compared with DSG treated with different sterilization techniques. No visible differences in the appearance and diameter of the fibers were observed after the sterilization treatments (Fig. S1 in Supplementary Information).

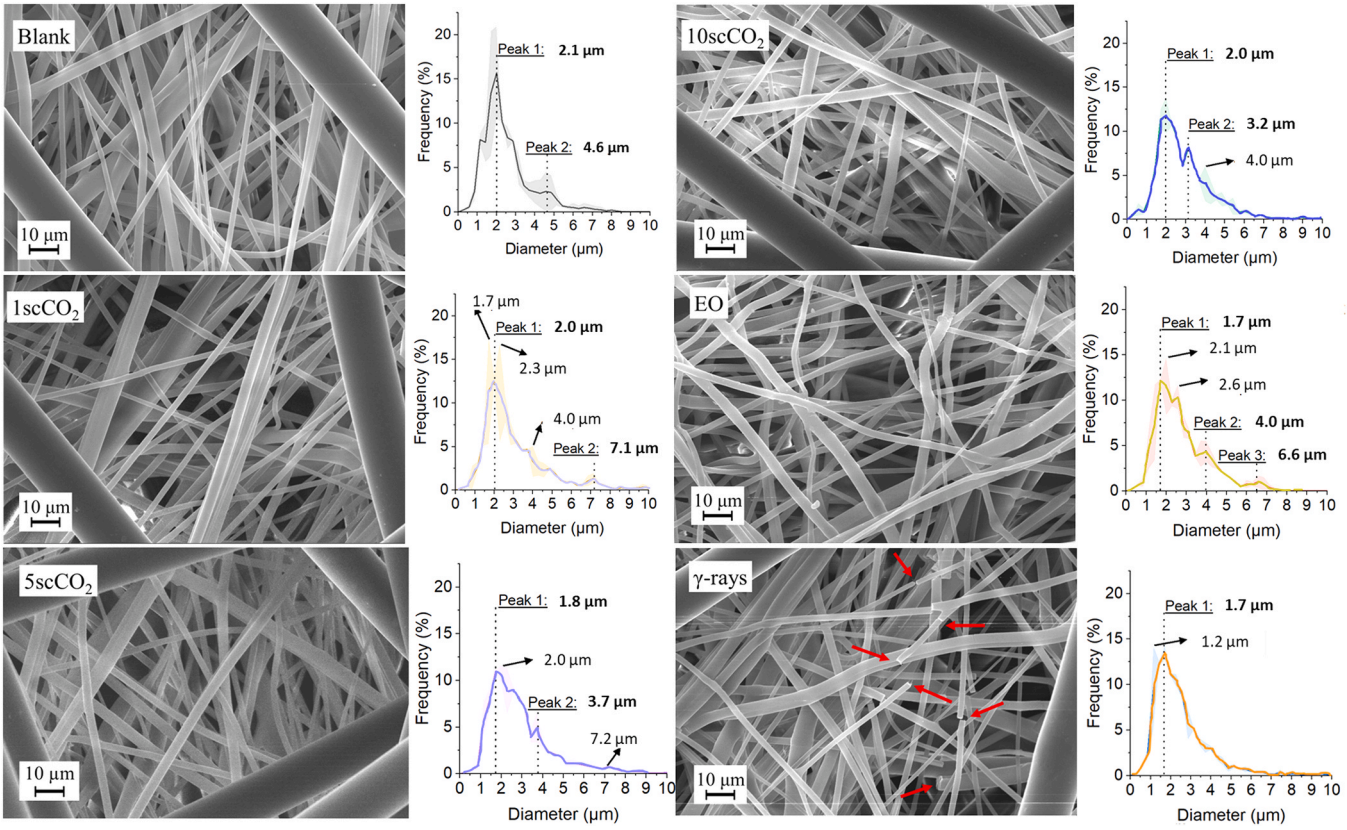

Fig. 1. SEM images of sterilized and control DSG and diameter distribution analysis of microfibers in DSG. Standard deviations were drawn with filled area. Red arrows in γ-rays image point to broken microfibers. For SEM images and diameter distribution analysis related to fibers, refer to Fig. S1 in Supplementary Information section.

Microfibers from *1scCO$_2$*, *5scCO$_2$*, *10scCO$_2$* and *EO* DSG samples did not suffer alterations. On the contrary, those of *γ-rays* showed relevant structural modifications with evident breakage (Fig. 1). Additional modifications on microfibers and fibers morphology were assessed by determining their diameter distributions from images of the external side of *SMMMS* fabrics (Fig. 1 and S2, respectively). Microfibers diameters seemed to be affected after every sterilization treatment, with shifts in the peak maximum from 2.1 μm towards lower values and with the appearance of new family peaks.

The chemical composition of the *SMMMS* fabric was evaluated by FTIR and DSC analyses. Results of FTIR spectroscopy analysis (Fig. 2) revealed no chemical alterations between the untreated and treated fabrics of the DSG. On one hand, Table 1 and Fig. 2 show that fibers/microfibers are made of isotactic polypropylene (iPP) since all peaks associated with this polymer were found in each sample. On the other hand, some bands associated with PE coating were observed: crosslinked PE at 1090 cm^{-1} and PE-crystallinity at 719 + 731 cm^{-1} [46–48]. Two additional bands were noticed at 782 and 755 cm^{-1}. The former could be a consequence of a linear low-density PE (LLDPE) like octane-1 and the latter can be attributed to CH_2 rocking vibrations of PP or PE branches [49–51].

DSC analyses were performed to analyze changes in the thermal events of DSG components after the different sterilization procedures (Table 2). The complete thermogram of the samples where these events can be found is showed in Fig. S3. The thermogram of the *Blank* DSG confirmed the melting peaks of both iPP and LLDPE at 160–167 °C and 108–112 °C, respectively [48,58,59]. The percentage of crystallinity of iPP was estimated from DSC thermograms by dividing the melting enthalpy ($\Delta H_{m,iPP}$) by the enthalpy of iPP with 100 % crystallinity ($\Delta H_{m,100\,\%} = 207\ J{\cdot}g^{-1}$ [58,59]). As LLDPE was a coating treatment over iPP, its peak had a small intensity. Therefore, the crystallinity variations of this polymer were determined by the peak ratio of FTIR spectra ($h_{719cm\text{-}1}/h_{731cm\text{-}1}$) rather than by using the melting enthalpy of LLDPE from DSC analysis. An increase in the absorbance band at 731 cm^{-1} (Fig. 2) indicates a higher PE crystallinity, whereas the peak ratio from 719 cm^{-1} to 731 cm^{-1} increases with the reduction of PE crystallinity [46,48]. Both polymers (i.e. iPP and LLDPE) suffered slight variations in their thermal behaviors depending on the applied sterilization method (Table 2). On one hand, *XscCO$_2$* and *EO* samples exhibited comparable T_m values for iPP, but a decrease of 3 °C after *γ-rays* sterilization. On the other hand, the T_m of LLDPE showed a decrease in T_m for each sterilization treatment compared to *Blank*, as well as a non-statistically significant increase in peak ratio (i.e. decreasing tendency in crystallinity). In *γ-rays* DSG sample, LLDPE underwent irregular variation for T_m and crystallinity, meaning that SMMMS fabrics were not

Table 1
Characteristic FTIR bands and vibration mode assignments for PP and PE polymers.

Band position (cm^{-1})	Vibration mode assignment	Polymer	Ref.
1167	Asymmetric stretching C−C Asymmetric rocking CH_3 Wagging CH	PP	[52,53]
1102	Vibration of isotactic PP	PP	[48,54,55]
1090	C-O stretching of crosslinked PE	PE	[48]
998	Asymmetric rocking CH_3	iPP	[52,53,56]
973	Asymmetric rocking CH_3 Asymmetric stretching C-C	PP	[52,53]
899	Asymmetric rocking CH_3 Asymmetric stretching C−C Symmetric stretching C-C	PP	[53]
841	Rocking CH_2	PP	[53,57]
809	Rocking CH_2	PP	[53,57]
782	Branches vibration of PE (Rocking CH_2 from LLDPE – Octene−1)	PE	[50]
731	Rocking CH_2 (Crystalline phase)	PE	[46–48]
719	Rocking CH_2 (Crystalline + Amorphous phase)	PE	[46–48]

Table 2
Thermal events (T_m and crystallinity) of iPP and LLDPE in DSG subjected to different sterilization treatments. Both parameters were measured three times for each polymer. The same letter indicates statistically homogeneous groups (p = 0.05).

DSG sample	T_m (°C)		Crystallinity iPP (%)	Peak ratio LLDPE
	iPP	LLDPE		
Blank	160.5 ± 0.3^{a}	109.3 ± 8.1$^{a'}$	45.0 ± 1.5^{d}	0.88 ± 0.05$^{c'}$
1scCO$_2$	160.8 ± 0.3^{a}	88.5 ± 5.0$^{b'}$	44.9 ± 0.4^{d}	0.96 ± 0.02$^{c'}$
5scCO$_2$	160.8 ± 0.2^{a}	90.7 ± 5.0$^{b'}$	44.9 ± 0.2^{d}	0.92 ± 0.04$^{c'}$
10scCO$_2$	160.9 ± 0.0^{b}	93.7 ± 5.4$^{b'}$	44.3 ± 0.8^{d,e}	0.90 ± 0.02$^{c'}$
EO	160.4 ± 0.1^{b}	97.4 ± 6.1$^{b'}$	44.8 ± 0.4^{d}	0.90 ± 0.05$^{c'}$
γ-rays	157.3 ± 0.2^{c}	104.9 ± 9.7$^{b'}$	42.3 ± 0.3^{e}	0.95 ± 0.11$^{c'}$

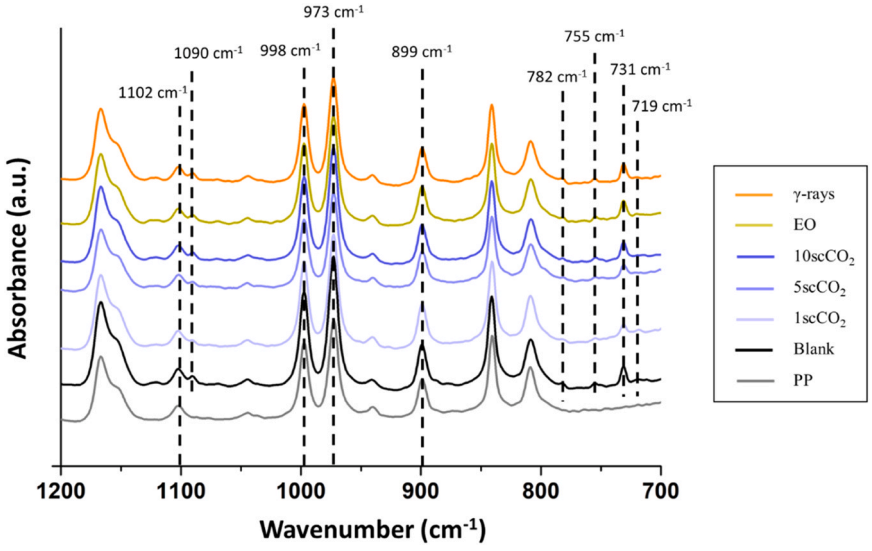

Fig. 2. FTIR spectra of control and sterilized DSG. Band intensities were normalized with the wavenumber at 2916 cm^{-1}. A non-woven fabric made of PP (17 g·m^{-2}) was used as a reference.

homogeneous on their surface.

3.3. Performance of the DSG before and after the different sterilization treatments

3.3.1. Water contact angle and hydrostatic pressure tests

Surgical clothing must not allow any droplet of fluid or solid particle to pass through them. This feature can be confirmed by WCA and hydrostatic pressure tests. The obtained WCA values were higher than 90° in all cases (Fig. 3A and S5). DSG treated with $scCO_2$ slightly increased (i.e. not statistically significant) their average WCA values compared to *Blank*. DSG chemically sterilized with EO maintained a similar WCA value, while *γ-rays* showed a lower average WCA. Regarding the average hydrostatic pressure tests, it was noticed that after $scCO_2$ and γ-rays treatments, the resistance of DSG to water penetration was higher than the resistance offered by the control sample (Fig. 3B). However, in the case of *EO*, there was a notable drop in water resistance, although its value was still above the required threshold value of 20 mbar and it did not present statistically significant differences with the other samples.

3.3.2. Tensile strength and bursting strength tests

Tensile strength testing offers important information about the mechanical properties of a fabric [60]. By applying controlled uniaxial tensile loading to the material, it is possible to measure its resistance to stretching and breaking. Bursting strength is the perpendicular force required to rupture a material by applying pressure until it bursts [61].

Tensile strength values obtained from the tests in longitudinal direction in the dry state (Fig. 4A) barely decreased after 1, 5 or 10 cycles of $scCO_2$. Conversely, in the wet state, these values increased with respect to *Blank*. In the case of EO sterilization the results follow the same trend, whereas after γ-rays treatment the tensile strength was reduced by approximately half in both dry and wet states.

In the lateral direction (Fig. 4B) and dry state, no differences were appreciated between *Blank* (43.91 N) and *XscCO₂* or *EO* samples. However, in the case of *γ-rays* sample, values were reduced to about half of those of *Blank*. In the wet state, tensile strength for *Blank* was 44.80 N, and while in the *1scCO₂* and *5scCO₂* samples this value slightly decreased, it raised for *10scCO₂*. In the case of EO sterilization, values also increased. As in longitudinal direction, *γ-rays* values were reduced to more than half compared with *Blank*.

Tensile strength measurements allowed the obtention of strain values of the sterilized DSG. Strain in longitudinal (Fig. 4C) and lateral (Fig. 4D) directions in the dry state showed no significant changes between the *Blank*, *1scCO₂* and *5scCO₂*. However, differences between *10scCO₂* and *Blank* are more pronounced and, with values for *EO* being similar to *10scCO₂*. In the wet state, longitudinal strain values obtained for the different *scCO₂* treatments and *EO* were similar, whereas *1scCO₂* and *5scCO₂* seemed to differ more from the *Blank* than *10scCO₂* and *EO* in case of the lateral strain. Again, *γ-rays* had remarkably lower strain than the rest of untreated and treated samples. Fig. S4 shows the stress-strain curves of the different samples for the two directions (longitudinal and lateral) and the two states (dry and wet) and no other variations different from those abovementioned were observed.

Finally, in the bursting strength test both in the dry and the wet states, *1scCO₂* did not show considerable variations with respect to the *Blank* in any side of the gown, external (Fig. 4E) or internal (Fig. 4F). These values were maintained or even improved for *5scCO₂* and *10scCO₂* on both sides of the DSG. The same happened after sterilization with EO. In the case of *γ-rays*, the results in the bursting strength tests did not accomplish the established requirements.

4. Discussion

$ScCO_2$ sterilization of DSG is explored in this work as a technological solution for their safe reuse and disposal. Previously, the effect of $scCO_2$ combined with a small quantity of H_2O_2 was proved effective in the sterilization of *B. pumilus* spore suspensions [24], less resistant than dry spores, whose destruction was later achieved at relevant levels by adding higher amounts of H_2O_2 [25]. Prior works pointed out that the interaction of CO_2 with certain polymers can alter their physical, thermal and mechanical properties, particularly under supercritical conditions [62,63]. Although previous works achieved the sterilization of similar polymers and even pieces of PPE without compromising the integrity of the material the influence of $scCO_2$ treatments on the properties and performance of polymers should be studied on a case-by-case basis [24,31]. For instance, in a prior study, the possibility of reusing or recycling several PPE components using $scCO_2$ was assessed [64]. This work concluded that PPE which are mainly composed of semicrystalline polymers (masks, gowns, shoe covers, etc.) were reusable.

The analysis of the SEM images allowed not only a qualitative evaluation of the DSG samples, but also the measurement of the diameter distribution of microfibers and fibers (Fig. 1 and S2). Microfibers sterilized by γ-rays showed significant fractures. In the literature, it was demonstrated that subjecting materials to γ-rays enhances its susceptibility to oxidation due to the generation of free radicals and ions that become trapped within the crystalline structure of the polymer [65]. This effect promotes the breakage of covalent bonds in the main chain of the polymer, resulting in a significant increase in the microfiber brittleness which could explain the fractures. By contrast, $scCO_2$ did not

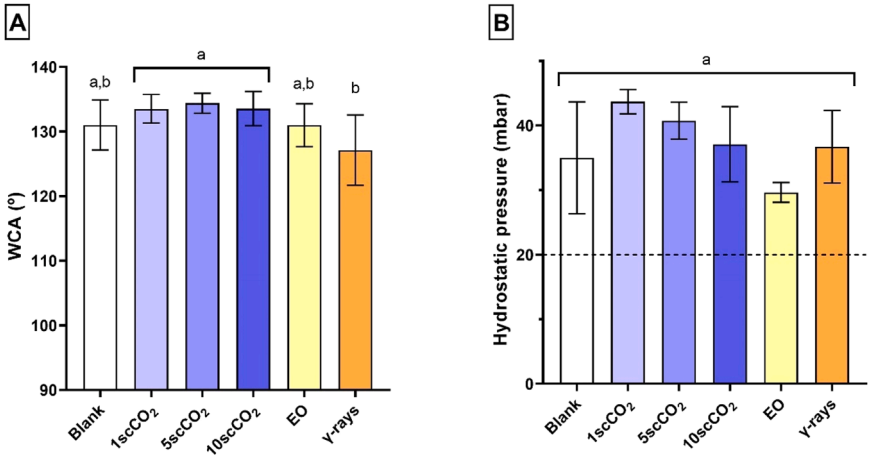

Fig. 3. (A) WCA values and (B) hydrostatic pressure test results (horizontal dashed line: standard performance requirement for DSG ≥ 20 mbar). The same letter indicates statistically homogeneous groups (p = 0.05).

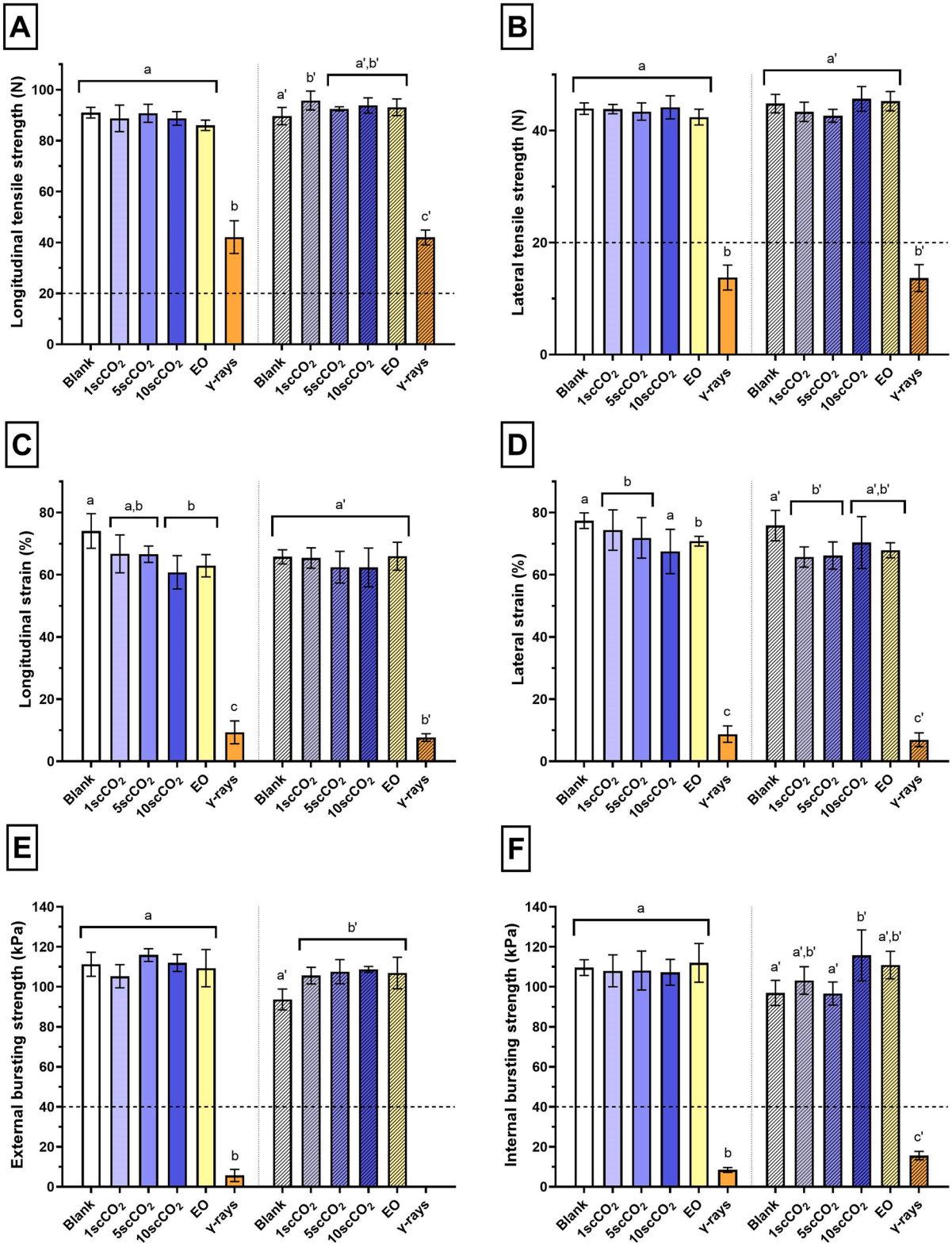

Fig. 4. Mechanical tests of DSG: (A) longitudinal tensile strength, (B) lateral tensile strength (horizontal dashed lines correspond to the standard performance requirement of 20 N), (C) longitudinal strain and (D) lateral strain obtained after the different sterilization treatments. Bursting strength applied to (E) external and (F) internal sides of the DSG samples (horizontal dashed lines correspond to the standard performance requirement of 40 kPa). In all cases, solid bars (located on the left side of the graphs) represent dry DSG, whereas stripped bars (located on the right side) refer to wet DSG. Same letter indicates statistically homogeneous groups ($p = 0.05$).

cause morphological changes in fibers and microfibers, even after 10 reprocessing cycles. Regarding the microfiber diameter distribution, the center of distribution for *EO* and *XscCO$_2$* underwent variations between 1.7 and 2.1 μm. Additionally, both EO and scCO$_2$ sterilization treatments induced a rise of secondary peaks towards microfibers with higher diameters than *Blank*. In *γ-rays*, the distribution shifted toward microfibers with lower diameters than *Blank*. In the case of fibers, all treatment results were similar to those of *Blank*, as observed both in SEM images and in the fiber diameter distribution. This suggests that in this case, even 10 cycles of scCO$_2$ sterilization are just as respectful as EO and γ-rays sterilization treatments.

No chemical changes on the SMMMS fabrics of DSG were caused by the sterilization treatments (Fig. 3) according to FTIR results, as all characteristic peaks associated with iPP, and those linked to the PE coating, were virtually unaltered in all cases (Table 1). Especially, the unaltered FTIR results of *10scCO$_2$* suggested that DSG fabrics are resistant to the oxidation that could be caused by H$_2$O$_2$.

The presence of iPP is confirmed by the characteristic bands at 1102 and 998 cm^{-1} , associated with the α-helix conformation of the isotactic chain, which allows it to be differentiated from atactic polypropylene (aPP) [56]. The similar intensity of 998 cm^{-1} band indicates that iPP structural order was not significantly altered after the sterilization treatment, and that the crystalline proportion of the polymer was maintained. Some studies have reported a partial absorption of CO$_2$ by iPP after being subjected to similar conditions (140 bar and 40 ºC for 30 min), which could cause small variations in crystallinity that lead to a decrease in stiffness and resistance to deformation [61,66]. However, other works pointed out that polymers without polar and flexible pendant groups are less susceptible to plasticizing agents [63]. In this work, no changes in crystallinity were perceived for samples treated with *scCO$_2$* or *EO*, while a significant reduction in crystallinity of 3 % was observed for the case of *γ-rays* samples. This reduction in crystallinity could cause the weakening of the fibers/microfibers and the consequent breakage that was clearly observed in the SEM images (Fig. 1) [65,67]. The relationship established between the calculated crystallinity percentages and the T$_m$ values is consistent with those experimental values found in the literature [68]. As the amount of LLDPE is very low, the impact of the different sterilization techniques on this polymer had to be evaluated in relative terms. Previous works reported that the CO$_2$ absorption by semicrystalline polymers can induce an increased crystallization as well as an increase in the T$_m$ and melting enthalpy, as also observed for T$_m$ in this work for the samples treated with scCO$_2$ (Table 1) [63]. While no differences in the crystallinity of LLDPE were observed in this work, all the sterilization treatments caused a slight decrease in the T$_m$ of this polymer.

While the crystallinity values of LLDPE did not provide particularly informative results, combining these results with the measurement of WCA is useful for assessing the impact of different sterilization treatments on the polymer functionality. WCA tests allowed the determination of the wettability and DSG demonstrated to be hydrophobic fabrics. The WCA of *EO* was similar to that of the control sample and *γ-rays* presented the lowest value, although the variability between the different gowns was almost unsignificant. The reduction of WCA in *γ-rays* could be attributed to oxidation of the polymers at the surface of the DSG, which would imply the formation of polar, hydrophilic groups [69]. Even though the WCA of *XscCO$_2$* and *Blank* samples were statistically the same, the average WCA of *XscCO$_2$* indicated that such samples were slightly more hydrophobic than the *Blank*. Previous studies have shown that scCO$_2$ treatment decreases the amount of hydrophilic functional groups of several materials, thus increasing hydrophobic ones [70–72]. The latter can explain the greater angles obtained on SMMMS fabrics of the DSG treated with scCO$_2$.

The hydrostatic pressure test was employed to measure water resistance to penetration under hydrostatic pressure according AATCC standard method 127–2017. Results showed that all samples exceeded a hydrostatic pressure of 20 mbar (about 20 cm H$_2$O or aqueous solutions like body fluids). Water resistance of DSG depends on the manufacturer and other works report values ranging from 30 to 52 mbar, which are in a wider range than the values obtained after all the sterilization treatments herein tested [73,74]. scCO$_2$ sterilization provided the most outstanding results of the three techniques since the DSG samples treated in that manner resulted in the most resistant against water penetration. This resistance decreased as the number of scCO$_2$ cycles increased, being always above the *Blank* average value. *γ-rays* samples also showed better results than the control (*Blank)* sample. However, EO sterilization was the only technique after which the resistance to water penetration was notably reduced. In the case of *γ-rays*, a divergent behavior is observed: while the thinner fibers break and crack, the thicker fibers maintain their rigidity, exhibiting residual structural resistance. Conversely, the enhancement in the pressure resistance exhibited by the DSG treated with scCO$_2$ could be related to two factors: firstly, the fibers maintain a rigidity comparable to that observed in the control samples, and secondly, highly hydrophobic surfaces, like the DSG samples sterilized by scCO$_2$, demonstrate a better resistance to water [75].

The tensile strength test was evaluated in dry and wet states, and in longitudinal and lateral directions. The standard performance requirement set by EN 13795–1:2019 establishes that the minimum supported strength is 20 N for commercial DSG. ScCO$_2$ (regardless of the number of cycles) and EO sterilization techniques surpassed such limit in both directions and states. The small variations in the tensile strength of the sterilized DSG with respect to the *Blank* could be expected as the crystallinity of the two polymers barely changed after any of these techniques [76]. On the contrary, *γ-rays* did not meet the requisite in lateral direction, which might be associated with the broken microfibers in that direction. A previous study demonstrated that tensile strength of LDPE did not experience statistically significant changes after being subjected to liquid CO$_2$ and to a mixture of CO$_2$ and H$_2$O$_2$ [77]. Such results are in line with the ones obtained in this work. In the case of strain values, only in the longitudinal direction in the wet state, there was a low variability between the samples, as the differences among all the samples (except for *γ-rays*) were not statistically significant. Nevertheless, in all other cases the variability was high, even between *XscCO$_2$* samples.

In regard to the bursting strength test, the standard performance requirement is established at 40 kPa in both dry and wet conditions. The test was conducted by measuring both the external and internal components of the gown, and the results followed closely in line with those of the tensile strength test. In comparison with the untreated sample, *1scCO$_2$*, *5scCO$_2$*, *10scCO$_2$* and *EO* not only surpassed the standard requirements but also achieved higher outcomes. In contrast, the DSG treated with γ-rays did not meet the standard below the requirement for dry or wet conditions. Other previous studies analyzed the effect of different ionizing radiation dosage on the breakage resistance of nonwoven medical materials, such as this DSG [78,79]. These studies also concluded that 35 kGy dosage was destructive to the fibers that compose the material, being particularly sensitive in bursting strength.

Radar charts in Fig. 5 summarize the operational conditions of each sterilization treatment, as well as the main results obtained in the performance tests of the sterilized DSG. Fig. 5A shows that EO sterilization is the one that requires the longest time and the highest temperature, whereas scCO$_2$ sterilization is the technique that operates at the highest pressure (140 bar) and requires less time (5.5 h) than the other techniques. Moderate operating temperatures are needed for γ-rays (25 ºC) and scCO$_2$ (39 ºC) sterilization. In the performance radar chart (Fig. 5B) for the treated DSG, the sterilization techniques that reached the external boundary of the chart for the hydrostatic pressure, tensile strength (on both directions) and bursting strength (on both sides) tests, surpassed the requirements set by the relevant standards for all tests. Conversely, those that fall in the middle do not meet at least one of these requirements. Accordingly, it is concluded that only scCO$_2$ and EO sterilization techniques comply with all the standard performance requirements for the reuse of DSG.

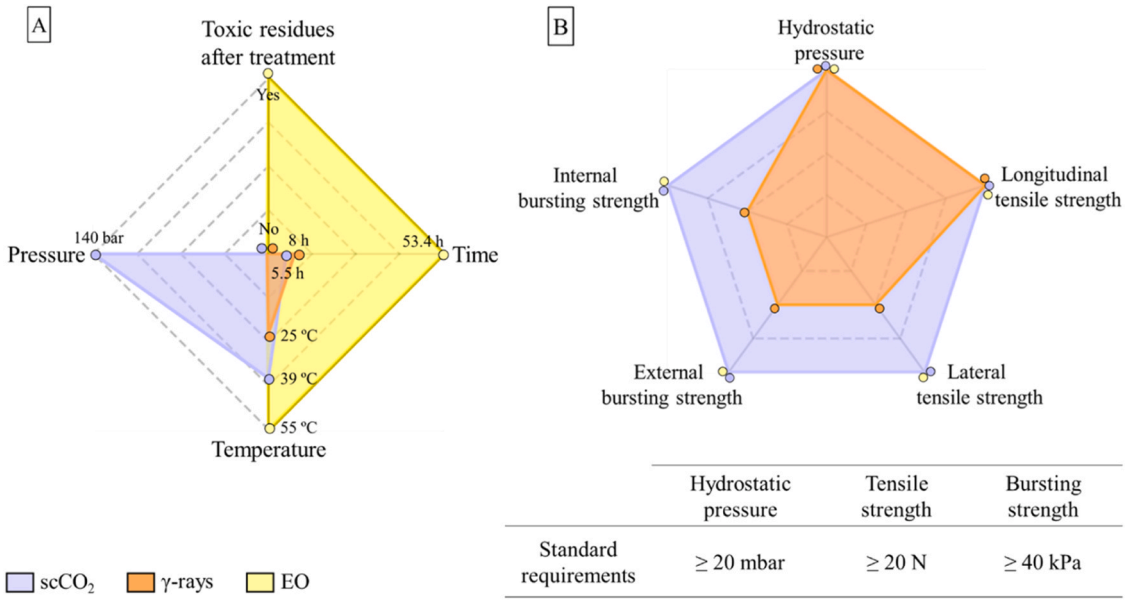

	Hydrostatic pressure	Tensile strength	Bursting strength
Standard requirements	≥ 20 mbar	≥ 20 N	≥ 40 kPa

Fig. 5. Radar charts applied to the sterilization of DSG. (A) Comparison of the operational conditions between the three sterilization techniques tested in this work. (B) Comparison of the DSG performance results obtained from the various tests conducted on the sterilized samples.

5. Conclusions

A successful sterilization method using $scCO_2$ has been developed for single-use, intact DSG. Such procedure constitutes a satisfactory and eco-friendly substitute to EO sterilization technique for DSG, as it allows multiple reprocessing of DSG (at least 10 cycles) without detriment to their physicochemical properties and functionality and valorizing CO_2. Furthermore, the conditions proposed to successfully sterilize dry spores of *B. pumilus* are relatively moderate in comparison to conventional sterilization methods. These consist of a temperature of 39 ºC, a pressure of 140 bar, a duration of 5.5 h, and a minimal quantity of additive. However, the duration of both the dynamic step and depressurization could be adjusted to minimize costs and promote scalability. DSG sterilized by EO showed in most cases similar results to those subjected to supercritical sterilization, except for the extended treatment and post-treatment periods (overall periods of *ca.* 2 days) before being reused, due to EO toxicity. γ-rays sterilization does not allow the reuse of *SMMMS* non-woven fabrics, as it caused structural damage that compromises their integrity and resulted in downgraded DSG mechanical performance that fails to meet the standard performance requirement set by the regulations. The satisfactory results with $scCO_2$ sterilization do not intend to propose DSG as an alternative to reusable SG but suggest the recovery and reuse of DSG that do not require washing steps before sterilization. The abovementioned results can be extended to other materials and endorse supercritical CO_2 sterilization as a potentially new benchmark for the reuse of PPE with efficacy demonstrated across up to 10 reprocessing cycles for DSG and with the added advantage of being environmentally friendly. Further studies on process scalability to industrial settings, process economic analysis, CO_2 recirculation and standardized operating and validation protocols will be the next steps for the evaluation of its technology transfer.

CRediT authorship contribution statement

Blanco-Vales María: Writing – review & editing, Writing – original draft, Methodology, Investigation. **Carracedo-Pérez María:** Writing – review & editing, Writing – original draft, Methodology, Investigation. **Sánchez-Ramírez Diego Omar:** Writing – review & editing, Methodology, Investigation. **Varesano Alessio:** Methodology, Funding acquisition. **Magariños Beatriz:** Writing – review & editing, Supervision, Methodology, Investigation, Funding acquisition, Conceptualization. **García-González Carlos A.:** Writing – review & editing, Writing – original draft, Supervision, Methodology, Investigation, Funding acquisition, Conceptualization. **López-Iglesias Clara:** Writing – review & editing, Writing – original draft, Supervision, Methodology, Investigation, Funding acquisition, Conceptualization.

Declaration of Competing Interest

The authors declare that they have no known competing financial interests or personal relationships that could have appeared to influence the work reported in this paper.

Acknowledgments

This work was funded by MICIU/AEI/10.13039/501100011033 [grants PID2023-151340OB-I00 and PDC2022-133526-I00], Xunta de Galicia [ED431C2022/2023], ERDF/EU and European Union NextGenerationEU/PRTR. C.L.-I. acknowledges Xunta de Galicia for a post-doctoral fellowship [ED481B-2021-008]. This study received funding from the European Union – NextGenerationEU, Missione 4 Componente 2, CUP B53C22004100001 within the MICS (Made in Italy -Circular Sustainable) project. Work carried out in the framework of the ECO-AERoGELS COST Innovators' Grant (ref. IG18125) and funded by the European Commission.

Appendix A. Supporting information

Supplementary data associated with this article can be found in the online version at doi:10.1016/j.jece.2025.116978.

Data availability

Data will be made available on request.

References

[1] D. Silva, et al., Gamma radiation for sterilization of textile based materials for personal protective equipment, Polym. Degrad. Stab. 194 (2021) 109750, https://doi.org/10.1016/j.polymdegradstab.2021.109750.

[2] A. Yap, et al., A mixed-methods study on end-user perceptions of transitioning to reusable surgical gowns, Surg. Open Sci. 11 (2023) 33–39, https://doi.org/10.1016/j.sopen.2022.10.003.

[3] S.M. Lee, D. Lee, Effective medical waste management for sustainable green healthcare, Art. no. 22, Int. J. Environ. Res. Public Health 19 (22) (2022), https://doi.org/10.3390/ijerph192214820.

[4] 'Water, sanitation and hygiene in health care facilities: Status in low- and middle-income countries and way forward'. Accessed: May 21, 2024. [Online]. Available: ⟨https://www.who.int/publications-detail-redirect/9789241508476⟩.

[5] 'Medical Gowns', FDA. Accessed: Apr. 22, 2024. [Online]. Available: ⟨https://www.fda.gov/medical-devices/personal-protective-equipment-infection-control/medical-gowns⟩.

[6] A. Burguburu, C. Tanné, K. Bosc, J. Laplaud, M. Roth, M. Czyrnek-Delêtre, Comparative life cycle assessment of reusable and disposable scrub suits used in hospital operating rooms, Clean. Environ. Syst. 4 (2022) 100068, https://doi.org/10.1016/j.cesys.2021.100068.

[7] A. Agrawal and S. Kosgi, Healthcare Access. BoD – Books on Demand, 2022.

[8] E. Vozzola, M. Overcash, E. Griffing, An environmental analysis of reusable and disposable surgical gowns, AORN J. 111 (3) (2020) 315–325, https://doi.org/10.1002/aorn.12885.

[9] M. Overcash, A comparison of reusable and disposable perioperative textiles: sustainability state-of-the-art 2012, Anesth. Analg. 114 (5) (2012) 1055, https://doi.org/10.1213/ANE.0b013e31824d9cc3.

[10] 'How Are Surgical Gowns Regulated? - Knowledge'. Accessed: Mar. 25, 2025. [Online]. Available: ⟨http://www.hbwanli.com/info/how-are-surgical-gowns-regulated-102759006.html⟩.

[11] 'Medical devices old - European Commission'. Accessed: Apr. 07, 2025. [Online]. Available: ⟨https://single-market-economy.ec.europa.eu/single-market/european-standards/harmonised-standards/medical-devices-old_en⟩.

[12] M.J. Alfa, Medical-device reprocessing, Infect. Control Hosp. Epidemiol. 21 (8) (2000) 496–498, https://doi.org/10.1086/501792.

[13] B.K. Behera, H. Arora, Surgical Gown: A Critical Review, J. Ind. Textiles 38 (3) (2009) 205–231, https://doi.org/10.1177/1528083708091251.

[14] W.A. Rutala, D.J. Weber, Sterilization of 20 billion medical devices by ethylene oxide (ETO): consequences of ETO closures and alternative sterilization technologies/solutions, Am. J. Infect. Control 51 (11) (2023) A82–A95, https://doi.org/10.1016/j.ajic.2023.01.020.

[15] G.C. Soares, et al., Supercritical CO_2 technology: the next standard sterilization technique? Mater. Sci. Eng. C. 99 (2019) 520–540, https://doi.org/10.1016/j.msec.2019.01.121.

[16] L.P. López Anaya, 'Óxido de etileno, utilización como agente esterilizante y riesgos para la salud del personal sanitario', Rev. CES Salud Pública 5 (2) (2014) 154–162.

[17] C.K. Herczeg, J. Song, Sterilization of polymeric implants: challenges and opportunities, ACS Appl. Bio Mater. 5 (11) (2022) 5077–5088, https://doi.org/10.1021/acsabm.2c00793.

[18] Z. Dai, J. Ronholm, Y. Tian, B. Sethi, X. Cao, Sterilization techniques for biodegradable scaffolds in tissue engineering applications, J. Tissue Eng. 7 (2016), https://doi.org/10.1177/2041731416648810, 2041731416648810.

[19] P. Nikolai, B. Rabiyat, A. Aslan, A. Ilmutdin, Supercritical CO_2: properties and technological applications - a review, J. Therm. Sci. 28 (3) (2019) 394–430, https://doi.org/10.1007/s11630-019-1118-4.

[20] N. Ribeiro, et al., A new era for sterilization based on supercritical CO_2 technology, J. Biomed. Mater. Res. Part B Appl. Biomater. 108 (2) (2020) 399–428, https://doi.org/10.1002/jbm.b.34398.

[21] M. Oulé, D. Michael, J. Arul, Microbicidal effect of pressurized CO_2 and the influence of sensitizing additives, Eur. J. Sci. Res. 41 (2010) 570–582.

[22] J.A. Daniels, R. Krishnamurthi, S.S.H. Rizvi, A review of effects of carbon dioxide on microbial growth and food quality, J. Food Prot. 48 (6) (1985) 532–537, https://doi.org/10.4315/0362-028X-48.6.532.

[23] N.M. Dixon, D.B. Kell, The inhibition by CO_2 of the growth and metabolism of micro-organisms, J. Appl. Bacteriol. 67 (2) (1989) 109–136, https://doi.org/10.1111/j.1365-2672.1989.tb03387.x.

[24] V. Santos-Rosales, et al., Supercritical CO_2 sterilization: an effective treatment to reprocess FFP3 face masks and to reduce waste during COVID-19 pandemic, Sci. Total Environ. 826 (2022) 154089, https://doi.org/10.1016/j.scitotenv.2022.154089.

[25] M. Carracedo-Pérez, I. Ardao, C. López-Iglesias, B. Magariños, C.A. García-González, Direct and green production of sterile aerogels using supercritical fluid technology for biomedical applications, J. CO2 Util. 86 (2024) 102891, https://doi.org/10.1016/j.jcou.2024.102891.

[26] F. Scognamiglio, et al., Effects of supercritical carbon dioxide sterilization on polysaccharidic membranes for surgical applications, Carbohydr. Polym. 173 (2017) 482–488, https://doi.org/10.1016/j.carbpol.2017.06.030.

[27] V. Santos-Rosales, B. Magariños, C. Alvarez-Lorenzo, C.A. García-González, Combined sterilization and fabrication of drug-loaded scaffolds using supercritical CO_2 technology, Int. J. Pharm. 612 (2022) 121362, https://doi.org/10.1016/j.ijpharm.2021.121362.

[28] F. Zani, C. Veneziani, E. Bazzoni, L. Maggi, G. Caponetti, R. Bettini, Sterilization of corticosteroids for ocular and pulmonary delivery with supercritical carbon dioxide, Int. J. Pharm. 450 (1) (2013) 218–224, https://doi.org/10.1016/j.ijpharm.2013.04.055.

[29] M. Carracedo-Pérez, B. Magariños, C.A. García-González, 'Chapter 19 - Strategies for the sterilization of polymeric biomaterials', in: S. Thomas, A. Tharayil (Eds.), Polymeric Materials for Biomedical Implants, Woodhead Publishing, 2024, pp. 547–583, https://doi.org/10.1016/B978-0-323-99690-7.00020-0 (in Woodhead Publishing Series in Biomaterials.).

[30] D. Bennet, et al., Evaluation of supercritical CO_2 sterilization efficacy for sanitizing personal protective equipment from the coronavirus SARS-CoV-2, Sci. Total Environ. 780 (2021) 146519, https://doi.org/10.1016/j.scitotenv.2021.146519.

[31] L. Calvo, J. Casas, Sterilization of biological weapons in technical clothing and sensitive material by high-pressure CO_2 and water, Ind. Eng. Chem. Res. 57 (13) (2018) 4680–4687, https://doi.org/10.1021/acs.iecr.7b04794.

[32] J.L. Ellis, J.C. Titone, D.L. Tomasko, N. Annabi, F. Dehghani, Supercritical CO_2 sterilization of ultra-high molecular weight polyethylene, J. Supercrit. Fluids 52 (2) (2010) 235–240, https://doi.org/10.1016/j.supflu.2010.01.002.

[33] V. Santos-Rosales, et al., Supercritical CO_2 technology for one-pot foaming and sterilization of polymeric scaffolds for bone regeneration, Int. J. Pharm. 605 (2021) 120801, https://doi.org/10.1016/j.ijpharm.2021.120801.

[34] E. Shieh, A. Paszczynski, C.M. Wai, Q. Lang, R.L. Crawford, Sterilization of *Bacillus pumilus* spores using supercritical fluid carbon dioxide containing various modifier solutions, J. Microbiol. Methods 76 (3) (2009) 247–252, https://doi.org/10.1016/j.mimet.2008.11.005.

[35] J. Stael, M. Haspeslagh, I. Beekhuis, A. Martens, Steam sterilisation of disposable surgical gowns does not compromise resistance to wet microbial penetration, Vet. Rec. (2025) e5121, https://doi.org/10.1002/vetr.5121.

[36] M. Huang, M.K. Hasan, S.D. Pillai, M. Pharr, D. Staack, Electron beam technology for Re-processing of personal protective equipment, Radiat. Phys. Chem. 202 (2023) 110557, https://doi.org/10.1016/j.radphyschem.2022.110557.

[37] H.K. Ruiz, A. Cabañas, L. Calvo, Sterilisation and virus SARS-CoV-2 inactivation in personal protective equipment with supercritical CO_2, J. Ind. Eng. Chem. (2025), https://doi.org/10.1016/j.jiec.2025.01.041.

[38] 'UNE-EN ISO 11140-1:2015 Esterilización de productos para atenc…' Accessed: Mar. 25, 2025. [Online]. Available: ⟨https://www.une.org/encuentra-tu-norma/busca-tu-norma/norma?c=N0054921⟩.

[39] 'ISO 11135:2014', ISO. Accessed: Jul. 03, 2024. [Online]. Available: ⟨https://www.iso.org/standard/56137.html⟩.

[40] 'UNE-EN ISO 11137-1:2015/A2:2020 | Normas AENOR'. Accessed: Jul. 03, 2024. [Online]. Available: ⟨https://tienda.aenor.com/norma-une-en-iso-11137-1-2015-a2-2020-n0064443⟩.

[41] 'AATCC'. Accessed: Jan. 17, 2025. [Online]. Available: ⟨https://members.aatcc.org/store/tm127/535/⟩.

[42] 'UNE-EN 29073-3:1993 Textiles. Métodos de ensayo para los no te…' Accessed: Jan. 17, 2025. [Online]. Available: ⟨https://www.une.org/encuentra-tu-norma/busca-tu-norma/norma?c=N0011205⟩.

[43] 'UNE-EN ISO 13938-1:2020 Textiles. Propiedades del estallido de…' Accessed: Jan. 17, 2025. [Online]. Available: ⟨https://www.une.org/encuentra-tu-norma/busca-tu-norma/norma?c=N0064444⟩.

[44] L. Garcia-Gonzalez, et al., High pressure carbon dioxide inactivation of microorganisms in foods: the past, the present and the future, Int. J. Food Microbiol. 117 (1) (2007) 1–28, https://doi.org/10.1016/j.ijfoodmicro.2007.02.018.

[45] D. Venkataraman, E. Shabani, J.H. Park, Advancement of nonwoven fabrics in personal protective equipment Materials 16 (11) (2023), Art. no. 11, doi:10.3390/ma16113964.

[46] M.J. Cran, S.W. Bigger, Quantitative analysis of polyethylene blends by fourier transform infrared spectroscopy, Appl. Spectrosc. 57 (8) (2003) 928–932, https://doi.org/10.1366/000370203322258887.

[47] I. Noda, A.E. Dowrey, C. Marcott, J.L. Haynes, C. Marcott, Group frequency assignments for major infrared bands observed in common synthetic polymers BT, Phys. Prop. Polym. Handb. (2007) 395–406.

[48] C. Signoret, A.-S. Caro-Bretelle, J.-M. Lopez-Cuesta, P. Ienny, D. Perrin, MIR spectral characterization of plastic to enable discrimination in an industrial recycling context: II. Specific case of polyolefins, Waste Manag. 98 (2019) 160–172, https://doi.org/10.1016/j.wasman.2019.08.010.

[49] M.C. Harvey, A.D. Ketley, The infrared identification of short-chain branches in polyolefins, J. Appl. Polym. Sci. 5 (15) (1961) 247–250, https://doi.org/10.1002/app.1961.070051501.

[50] A. Prasad, A quantitative analysis of low density polyethylene and linear low density polyethylene blends by differential scanning calorimetery and fourier transform infrared spectroscopy methods, Polym. Eng. Sci. 38 (10) (1998) 1716–1728, https://doi.org/10.1002/pen.10342.

[51] B. Smith, The infrared spectra of polymers ii: polyethylene 36 (2021) 24–29, doi:10.56530/spectroscopy.xp7081p7.

[52] J. Fang, L. Zhang, D. Sutton, X. Wang, T. Lin, Needleless melt-electrospinning of polypropylene nanofibres, J. Nanomater. (1) (2012) 382639, https://doi.org/10.1155/2012/382639.

[53] R. Morent, N. De Geyter, C. Leys, L. Gengembre, E. Payen, Comparison between XPS- and FTIR-analysis of plasma-treated polypropylene film surfaces, Surf. Interface Anal. 40 (3–4) (2008) 597–600, https://doi.org/10.1002/sia.2619.

[54] J.M. Chalmers, M.W. Mackenzie, H.A. Willis, H.G.M. Edwards, J.S. Lees, D.A. Long, FTIR spectroscopic studies of isotactic polypropylene films under stress, Spectrochim. Acta Part A Mol. Spectrosc. 47 (12) (1991) 1677–1683, https://doi.org/10.1016/0584-8539(91)80005-4.

[55] P.C. Painter, M. Watzek, J.L. Koenig, Fourier transform infra-red study of polypropylene, Polymer 18 (11) (1977) 1169–1172, https://doi.org/10.1016/0032-3861(77)90114-8.

[56] R.A. Ozzetti, A.P. De Oliveira Filho, U. Schuchardt, D. Mandelli, Determination of tacticity in polypropylene by FTIR with multivariate calibration, J. Appl. Polym. Sci. 85 (4) (2002) 734–745, https://doi.org/10.1002/app.10633.

[57] M.S. Sevegney, R.M. Kannan, A.R. Siedle, P.A. Percha, FTIR spectroscopic investigation of thermal effects in semi-syndiotactic polypropylene, J. Polym. Sci. Part B Polym. Phys. 43 (4) (2005) 439–461, https://doi.org/10.1002/polb.20334.

[58] 'PP (isotactic): Polypropylene', NETZSCH - Analyzing and Testing. Leading in Thermal Analysis, Rheology and Fire Testing. Accessed: Jul. 04, 2024. [Online]. Available: ⟨https://analyzing-testing.netzsch.com/en/polymers-netzsch-com/commodity-thermoplastics/pp-isotactic-polypropylene⟩.
[59] 'Measurement of Tg of Polypropylene Using the Double-Furnace DSC| PerkinElmer'. Accessed: Jul. 04, 2024. [Online]. Available: ⟨https://www.perkinelmer.com/es/libraries/app_010032_01_measurement_of_tg_of_polypropylene_using_the_double_furnace_dsc⟩.
[60] 'Development of Models to Predict Tensile Strength of Cotton Woven Fabrics'. Accessed: Nov. 26, 2024. [Online]. Available: ⟨https://journals.sagepub.com/doi/epdf/10.1177/155892501100600407⟩.
[61] K.M. Elias, M.O. Rahman, H.M.Z. Hossain, Predicting bursting strength behavior of weft knitted fabrics using various percentages of cotton, polyester, and spandex fibers, J. Text. Sci. Technol. 9 (4) (2023), https://doi.org/10.4236/jtst.2023.94019. Art. no. 4v,.
[62] Y.-T. Shieh, J.-H. Su, G. Manivannan, P.H.C. Lee, S.P. Sawan, W. Dale Spall, Interaction of supercritical carbon dioxide with polymers. I. Crystalline polymers, J. Appl. Polym. Sci. 59 (4) (1996) 695–705, https://doi.org/10.1002/(SICI)1097-4628(19960124)59:4< 695::AID-APP15> 3.0.CO;2-P.
[63] L. Ansaloni, B. Alcock, T.A. Peters, Effects of CO2 on polymeric materials in the CO_2 transport chain: a review, Int. J. Greenh. Gas. Control 94 (2020) 102930, https://doi.org/10.1016/j.ijggc.2019.102930.
[64] H.K. Ruiz, J.M. Gómez-Salazar, L. Calvo, A. Cabañas, Characterisation of plastic-based sanitary personal protective equipment following supercritical CO_2 sterilisation: a reuse strategy, J. CO2 Util. 92 (2025) 103029, https://doi.org/10.1016/j.jcou.2025.103029.
[65] C. Maier, T. Calafut, '2 - Morphology and Commercial Forms, in: C. Maier, T. Calafut (Eds.), Polypropylene, William Andrew Publishing, in Plastics Design Library., Norwich, NY, 1998, pp. 11–25, https://doi.org/10.1016/B978-188420758-7.50007-2.
[66] M. Champeau, J.-M. Thomassin, C. Jérôme, T. Tassaing, In situ FTIR micro-spectroscopy to investigate polymeric fibers under supercritical carbon dioxide: CO_2 sorption and swelling measurements, J. Supercrit. Fluids 90 (2014) 44–52, https://doi.org/10.1016/j.supflu.2014.03.006.
[67] S. As Alariqi, A. A Mutair, Effect of different sterilization methods on biodegradation of biomedical polypropylene, J. Environ. Anal. Toxicol. 6 (3) (2016) 1–7, https://doi.org/10.4172/2161-0525.1000373.
[68] R. Paukkeri, A. Lehtinen, Thermal behaviour of polypropylene fractions: 1. Influence of tacticity and molecular weight on crystallization and melting behaviour, Polymer 34 (19) (1993) 4075–4082, https://doi.org/10.1016/0032-3861(93)90669-2.
[69] S.-Y. Jo, et al., Degradation behavior of poly (l-lactide-co-glycolide) films through gamma-ray irradiation, Radiat. Phys. Chem. 81 (7) (2012) 846–850, https://doi.org/10.1016/j.radphyschem.2012.03.013.
[70] C. Tsioptsias, C. Panayiotou, Thermal stability and hydrophobicity enhancement of wood through impregnation with aqueous solutions and supercritical carbon dioxide, J. Mater. Sci. 46 (16) (2011) 5406–5411, https://doi.org/10.1007/s10853-011-5480-1.
[71] T.T.B. Le, A. Striolo, D.R. Cole, Supercritical CO_2 effects on calcite wettability: a molecular perspective, J. Phys. Chem. C. 124 (34) (2020) 18532–18543, https://doi.org/10.1021/acs.jpcc.0c03210.
[72] H. Lee, et al., Diffusivity and hydrophobic hydration of hydrocarbons in supercritical CO_2 and aqueous brine, RSC Adv. 10 (62) (2020) 37938–37946, https://doi.org/10.1039/D0RA06499H.
[73] M. McQuerry, E. Easter, A. Cao, Disposable versus reusable medical gowns: a performance comparison, Am. J. Infect. Control 49 (5) (2021) 563–570, https://doi.org/10.1016/j.ajic.2020.10.013.
[74] 'Prediction of Hydrostatic Pressure and Blood Penetration of Medical Protective Clothing'. Accessed: Jan. 09, 2025. [Online]. Available: ⟨https://journals.sagepub.com/doi/epdf/10.1177/155892501601100104⟩.
[75] G. Wu, Y. Zhao, D. Ge, Y. Zhao, L. Yang, S. Yang, Highly robust, pressure-resistant superhydrophobic coatings from monolayer assemblies of chained nanoparticles, Adv. Mater. Interfaces 8 (2) (2021) 2000681, https://doi.org/10.1002/admi.202000681.
[76] J.-B. Bao, T. Liu, L. Zhao, G.-H. Hu, Carbon dioxide induced crystallization for toughening polypropylene, Ind. Eng. Chem. Res. 50 (16) (2011) 9632–9641, https://doi.org/10.1021/ie200407p.
[77] A. Jiménez, et al., Compatibility of medical-grade polymers with dense CO_2, J. Supercrit. Fluids 42 (3) (2007) 366–372, https://doi.org/10.1016/j.supflu.2007.05.002.
[78] R.Y. Galimzyanova, M.S. Lisanevich, E.R. Rakhmatullina, Y.N. Khakimullin, Medical nonwovens: effects of radiation sterilization on bursting strength, Key Eng. Mater. 869 (2020) 101–106, https://doi.org/10.4028/www.scientific.net/KEM.869.101.
[79] E.R. Rakhmatullina, M.S. Lisanevich, R.Y. Galimzyanova, Y.N. Khakimullin, The effect of radiation sterilization on the stress-strain properties of non-woven materials-based on polypropylene, Mater. Sci. Forum 992 (2020) 403–408, https://doi.org/10.4028/www.scientific.net/MSF.992.403.